Published for SISSA by Springer

Received: *March 4, 2026*
Revised: *March 13, 2026*
Accepted: *March 19, 2026*
Published: *May 8, 2026*

Search for a massless particle beyond the Standard Model in the $\Xi^0 \to \Lambda +$ invisible decay

The BESIII collaboration

Full author list at the end of the paper

E-mail: besiii-publications@ihep.ac.cn

Abstract: A search for a massless beyond-standard-model particle is performed in the decay $\Xi^0 \to \Lambda +$ invisible using $(1.0087 \pm 0.0044) \times 10^{10}$ J/ψ events collected with the BESIII detector at the BEPCII collider. No significant signal is observed and the upper limit on the branching fraction $\mathcal{B}(\Xi^0 \to \Lambda +$ invisible$)$ is set to be 2.3×10^{-4} at the 90% confidence level. This is the first search for a flavor-changing neutral current process with missing energy in Ξ^0 decays. Throughout this paper, charge-conjugate processes are always implied.

Keywords: Dark Matter, e^+-e^- Experiments, Branching fraction

ArXiv ePrint: 2603.03199

https://doi.org/10.1007/JHEP05(2026)073

JHEP05(2026)073

Contents

JHEP05(2026)073

1 Introduction

The flavor-changing neutral-current (FCNC) transitions $s \to d\bar{\nu}\nu$ are loop-induced and Glashow-Iliopoulos-Maiani (GIM) suppressed in the Standard Model (SM), with the expected branching fractions (BFs) below 10^{-11} [1]. If new invisible particles beyond the SM contribute, the BFs for some FCNC hyperon decays could be enhanced to 10^{-4} [2]. The search for such decays is therefore a sensitive probe for new physics (NP). NP particles such as the QCD axion or the dark photon could contribute to the FCNC decay $\Xi^0 \to \Lambda +$ invisible via tree-level or one-loop processes, as shown in figure 1.

The QCD axion is predicted by the Peccei-Quinn mechanism to resolve the strong CP problem [3–6]. The QCD axion mass scales inversely with its decay constant, f_a, which is constrained to be much greater than 10^6 GeV [7]. Consequently, the mass of the axion is expected to be significantly below the electronvolt scale. In this regime, the axion lifetime exceeds the age of the Universe, so it is a viable dark matter (DM) candidate [8–10]. In FCNC transitions relevant for axion searches, hyperon decays such as $\Xi^0 \to \Lambda +$ invisible could provide good sensitivity to specific couplings between the axion and quarks [11]. The possibility of a long-range gauge force associated with DM is considered, in the form of a new unbroken abelian field, which has been termed the $\mathrm{U}(1)_D$ dark photon, denoted as γ' [12–15]. If the $\mathrm{U}(1)_D$ symmetry remains unbroken, its associated gauge boson will not acquire any mass. Although a massless dark photon lacks direct couplings to SM fermions, it can still induce FCNC processes through higher-dimensional operators.

In this paper, we search for the beyond-standard-model massless particle in the two-body decay $\Xi^0 \to \Lambda +$ invisible, where the Ξ^0 candidate is identified by tagging a $\bar{\Xi}^0$ decaying to $\bar{\Lambda}\pi^0$ on the recoiling side. We employ approximately 10 million $\Xi^0\bar{\Xi}^0$ pairs from

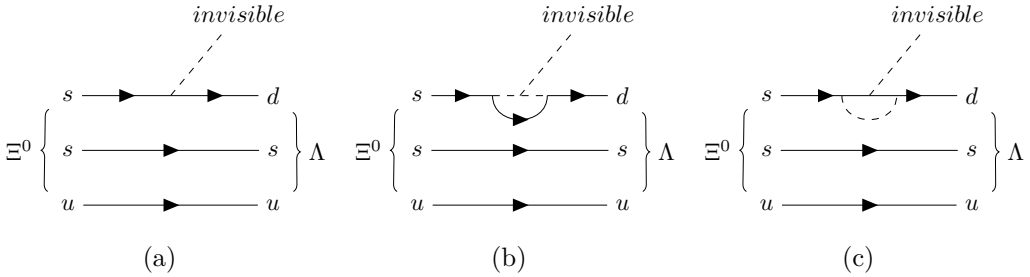

Figure 1. The possible Feynman diagrams for decay $\Xi^0 \to \Lambda +$ invisible in NP models: (a) tree-level Feynman diagram (such as QCD axion) and (b)(c) one-loop Feynman diagrams (such as dark photon).

$(1.0087 \pm 0.0044) \times 10^{10}$ J/ψ events [16] recorded with the BESIII detector. Throughout this paper, charge-conjugate processes are always implied unless explicitly specified.

2 BESIII detector and Monte Carlo simulation

The BESIII detector [17] records symmetric e^+e^- collisions provided by the BEPCII storage ring [18] in the center-of-mass energy range from 1.84 to 4.95 GeV, with a peak luminosity of 1.1×10^{33} cm^{-2}s^{-1} achieved at $\sqrt{s} = 3.773$ GeV. BESIII has collected large data samples in this energy region [19–22]. The cylindrical core of the BESIII detector covers 93% of the full solid angle and consists of a helium-based multilayer drift chamber (MDC), a plastic scintillator time-of-flight system (TOF) and a CsI(Tl) electromagnetic calorimeter (EMC), which are all enclosed in a superconducting solenoidal magnet providing a 1.0 T magnetic field. The magnetic field was 0.9 T in 2012, corresponding to 11% of the total J/ψ data. The solenoid is supported by an octagonal flux-return yoke with resistive plate counter muon identification modules interleaved with steel. The charged-particle momentum resolution at 1 GeV/c is 0.5%, and the dE/dx resolution is 6% for electrons from Bhabha scattering. The EMC measures photon energies with a resolution of 2.5% (5%) at 1 GeV in the barrel (end-cap) region. The time resolution in the TOF barrel region is 68 ps, while that in the end-cap region is 110 ps. The end-cap TOF system was upgraded in 2015 using multigap resistive plate chamber technology, providing a time resolution of 60 ps, and this upgraded system was utilized for 87% of the data in this analysis [23–25].

The Monte Carlo (MC) simulated data samples are produced with a GEANT4-based [26] software package, which includes the geometric description of the BESIII detector [27–31] and the detector response, are used to determine detection efficiencies and to estimate backgrounds. The simulation models the beam energy spread and initial-state radiation in the e^+e^- annihilations with the generator KKMC [32, 33]. The inclusive MC sample includes both the J/ψ resonance production and the continuum processes simulated in KKMC [32, 33]. All particle decays are modeled with EVTGEN [34, 35] using BFs either taken from the Particle Data Group (PDG) [36], when available, or otherwise estimated with LUNDCHARM [37, 38]. Final-state radiation from charged final-state particles is incorporated using the PHOTOS package [39]. To obtain the tag efficiency of $\bar{\Xi}^0 \to \bar{\Lambda}\pi^0$, the single tag (ST) MC sample $J/\psi \to \Xi^0(\to \Lambda +$anything$)\bar{\Xi}^0(\to \bar{\Lambda}\pi^0)$ is generated according to its helicity decay

JHEP05(2026)073

amplitudes [40]. The signal MC sample for the decay $J/\psi \to \Xi^0(\to \Lambda + \text{invisible})\bar{\Xi}^0(\to \bar{\Lambda}\pi^0)$ is generated according to its helicity decay amplitudes, where the decay-asymmetry parameter of $\Xi^0 \to \Lambda + \text{invisible}$ is assumed to be the same as that of $\Xi^0 \to \Lambda\pi^0$ decay. The subsequent decays $\Lambda \to p\pi^-$, $\bar{\Lambda} \to \bar{p}\pi^+$ and $\pi^0 \to \gamma\gamma$ are generated with the phase space model.

3 Single tag event selection

The analysis is performed using the BESIII offline software system [41]. The signal $\Xi^0 \to \Lambda + \text{invisible}$ is searched for with $\Lambda \to p\pi^-$ from $\Xi^0\bar{\Xi}^0$ pairs at the center-of-mass energy of $\sqrt{s} = 3.097\,\text{GeV}$. The $\bar{\Xi}^0$ candidates reconstructed through the dominant decay mode $\bar{\Xi}^0 \to \bar{\Lambda}\pi^0$ are denoted as ST side, with $\mathcal{B}_{\bar{\Xi}^0\to\bar{\Lambda}\pi^0} = (99.524 \pm 0.012)\%$ from the PDG [36]. The recoiling system opposite to the ST side in the space is defined as the double tagged (DT) side and treated as the signal. The BF of the signal decay can be calculated as:

$$\mathcal{B}_{\Xi^0\to\Lambda+\text{invisible}} = \frac{N_{\text{DT}} \times \epsilon_{\text{ST}}}{N_{\text{ST}} \times \epsilon_{\text{DT}} \times \mathcal{B}_{\Lambda\to p\pi^-}}, \tag{3.1}$$

where N_{ST} (N_{DT}) is the observed ST (DT) yield, ϵ_{ST} (ϵ_{DT}) the corresponding detection efficiency, and $\mathcal{B}_{\Lambda\to p\pi^-} = (64.1 \pm 0.5)\%$ the BF of $\Lambda \to p\pi^-$ from the PDG [36].

Events are required to have zero net charge and at least two charged tracks. All charged tracks must be detected in the MDC within the range of $|\cos\theta| < 0.93$, where θ is the polar angle with respect to the axis of symmetry of the MDC. The distance of closest approach from the interaction point must be less than 20 cm along the beam direction.

Particle identification (PID) is applied by combining the measurements of $\mathrm{d}E/\mathrm{d}x$ in the MDC and the time-of-flight in the TOF to calculate the likelihoods $\mathcal{L}(h)$ for each hadron hypothesis $h = p, K, \pi$. The π candidates are required to satisfy $\mathcal{L}(\pi) > 0$, $\mathcal{L}(\pi) > \mathcal{L}(K)$, while the p candidates must satisfy $\mathcal{L}(p) > 0$, $\mathcal{L}(p) > \mathcal{L}(K)$ and $\mathcal{L}(p) > \mathcal{L}(\pi)$. Due to the low momenta of pions (less than $0.4\,\text{GeV}/c$) and protons (less than $0.9\,\text{GeV}/c$), the identification efficiencies for pions and protons exceed 99%, with misidentification probabilities less than 1%. At least one π candidate and one p candidate are required for each event.

Photon candidates are selected from showers deposited in the EMC with energies of $E_\gamma > 25\,\text{MeV}$ in the barrel ($|\cos\theta| < 0.80$) and $E_\gamma > 50\,\text{MeV}$ in the end-cap ($0.86 < |\cos\theta| < 0.92$). Showers must be separated from the extrapolated positions of any charged track by at least 10° (20° for the anti-proton track) and occur within 700 ns after the event start time. At least two photon candidates are required per event. The π^0 candidates are reconstructed by looping over all pairs of good photons and their invariant mass is required to lie in the range of $(0.115, 0.150)\,\text{GeV}/c^2$, which is approximately a $\pm 2\sigma$ window around the nominal mass of π^0. The $\chi^2_{\gamma\gamma}$ from a one-constraint (1C) kinematic fit constraining their invariant mass to the known π^0 mass [36] must be less than 25. The updated π^0 four-momentum from the 1C kinematic fit is used in later calculations.

The $\bar{\Lambda}$ candidates are reconstructed via the $\bar{p}\pi^+$ final state. Primary and secondary vertex fits are performed to all $\bar{p}\pi^+$ candidates, where the primary vertex is the production vertex of the $\bar{\Lambda}$ and the secondary vertex is its decay vertex. The χ^2 variables of primary and secondary vertex fits are both required to be less than 100. The decay length L divided by its uncertainty σ_L obtained from the secondary vertex fit must be greater than 2. The $\bar{p}\pi^+$

JHEP05(2026)073

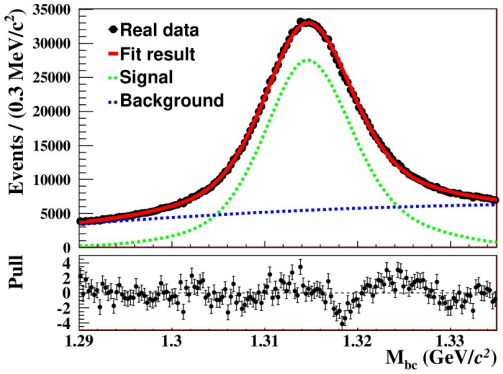

Figure 2. The fit on the $M_{\rm bc}$ from the ST side. The black dots with error bars represent the data and the red line represents the total fit, whose signal component is shown with the green dashed line and the background component with the blue dashed line. The bottom panel shows the pull values, defined as $Pull^i = \frac{N^i_{\rm data} - N^i_{\rm fit}}{\sigma^i_{\rm data}}$, where $N^i_{\rm data}$ is the number of data events in the i-th bin, $N^i_{\rm fit}$ is the corresponding total number of fitted events, and $\sigma^i_{\rm data}$ is the statistical uncertainty of the data.

invariant mass $M_{\bar{p}\pi^+}$, obtained after the secondary vertex fit, is required to lie within the interval $(1.111, 1.120)\,{\rm GeV}/c^2$, which is about a $\pm 3\sigma$ window around the nominal mass of Λ. The $\bar{\Lambda}$ candidates satisfying all the above requirements are designated as good $\bar{\Lambda}$ candidates. At least one good $\bar{\Lambda}$ candidate is required. The updated $\bar{\Lambda}$ four-momentum, obtained by the secondary vertex fit, is used in all subsequent steps.

The $\bar{\Xi}^0$ is reconstructed with the combination of $\bar{\Lambda}$ and π^0 candidates using their updated four-momentum after the fits. The best ST $\bar{\Xi}^0$ candidate is determined with minimum $\Delta E = |E_{\bar{\Lambda}\pi^0} - E_{\rm cms}/2|$ value from all possible $\bar{\Lambda}$ and π^0 combinations, where $E_{\bar{\Lambda}\pi^0}$ is the total energy of the $\bar{\Lambda}$ and π^0 candidates, and $E_{\rm cms}$ is the center-of-mass energy. $|M_{\bar{\Lambda}\pi^0} - M_{\bar{\Xi}^0_{\rm PDG}}| < 0.02\,{\rm GeV}/c^2$ is required for $\bar{\Xi}^0$ candidate, where $M_{\bar{\Lambda}\pi^0}$ is the invariant mass of $\bar{\Lambda}$ and π^0, and $M_{\bar{\Xi}^0_{\rm PDG}}$ is the nominal mass of $\bar{\Xi}^0$ from the PDG [36]. The ST yield is extracted from a binned maximum likelihood fit to the distribution of $M_{\rm bc}$, defined as

$$M_{\rm bc} = \sqrt{E^2_{\rm cms}/4c^4 - |\vec{P}|^2_{\bar{\Lambda}\pi^0}/c^2}, \tag{3.2}$$

where $\vec{P}_{\bar{\Lambda}\pi^0}$ is the total momentum of the $\bar{\Lambda}$ and π^0 candidates. The signal process $J/\psi \to \bar{\Xi}^0(\to \Lambda\pi^0)\Xi^0(\to X)$ is dominant, while the background distribution is smooth and well described by a polynomial. The signal shape is described by the MC-simulated shape convolved with a Gaussian function, which represents the resolution difference between the data and MC simulation. A second-order Chebyshev polynomial describes the background shape in the fit. We obtain $(1.254 \pm 0.004) \times 10^6$ ST events in the signal region, as shown in figure 2, where the uncertainty is statistical only.

The ST detection efficiencies are evaluated using the signal MC sample, and are found to be $(8.15 \pm 0.01)\%$. As a consistency check, the BF of $J/\psi \to \bar{\Xi}^0\Xi^0$ is measured to be $(1.212 \pm 0.004) \times 10^{-3}$ according to the observed ST yield and the corresponding ST efficiency, which is consistent with the previous BESIII measurements [40, 42].

JHEP05(2026)073

4 Double tag event selection

After a $\bar{\Xi}^0$ candidate is identified on the ST side, the signal decay $\Xi^0 \to \Lambda +$ invisible is probed in the DT side, where the final state consists of p, π^- and an invisible particle. Exactly two additional charged particles are required, and they must be identified as a proton and a pion, which are used to reconstruct the Λ candidate. The selection requirements for protons and pions on the DT side are the same as those for the ST side, as introduced in section 3.

Two two-constraint (2C) kinematic fits are performed under the hypothesis of $J/\psi \to p\bar{p}\pi^+\pi^-\pi^0 +$ invisible, which impose four-momentum conservation and assign the π^0 mass to the photon pair. In the first 2C kinematic fit, the invisible particle is assumed to be massless, while in the second fit, it is assigned the nominal π^0 mass. The $\chi^2_{\rm 2C}$, obtained from the first 2C kinematic fit, must be less than 8.5. The four-momenta of the invisible particle, p and π^- candidates on the DT side are obtained by this fit. To suppress the background from $\Xi^0 \to \Lambda\pi^0$, the $\chi^2_{\rm 2C\pi^0}$ of the second 2C kinematic fit must be greater than $\chi^2_{\rm 2C}$. The invariant mass of $p\pi^-$ and the invisible particle, denoted as $M_{p\pi^-+\rm inv.}$, is required to be in the range of $(1.310, 1.322)\,\mathrm{GeV}/c^2$. For the background processes $\Xi^0 \to \Lambda\gamma$ and $\Xi^0 \to \Lambda\pi^0$, the missing photon carries the energy and momentum. Typically, the missing photon is either outside the detector ($|\cos\theta| > 0.92$) or located in the gaps between the barrel and the two end caps ($0.80 < |\cos\theta| < 0.86$). Therefore, the polar angle of the invisible particle must satisfy $|\cos\theta_{\rm inv.}| < 0.8$. To suppress the background $J/\psi \to \Sigma^0(\to \Lambda\gamma)\bar{\Sigma}^0(\to \bar{\Lambda}\gamma)$, the missing momentum $|\vec{P}_{\rm inv.}|$ from the first 2C kinematic fit, is required to be $|\vec{P}_{\rm inv.}| > 0.15\,\mathrm{GeV}/c$.

If the number of photon candidates exceeds two, a five-constraint (5C) kinematic fit is performed under the hypothesis of $J/\psi \to p\bar{p}\pi^+\pi^-\pi^0\gamma$, where the γ is one of the photons not originating from the π^0 on the ST side. We loop over all such photons and require the minimum $\chi^2_{\rm 3\gamma}$ to be greater than 1000. In addition, if the number of photon candidates exceeds three, a six-constraint (6C) kinematic fit is performed under the hypothesis of $J/\psi \to p\bar{p}\pi^+\pi^-\pi^0\gamma\gamma$, where the $\gamma\gamma$ are two photons not originating from the π^0 on the ST side. We loop over all such photons and require the minimum $\chi^2_{\rm 4\gamma}$ to be greater than 1000.

The selection criteria on $M_{\rm bc}$, $\chi^2_{\rm 2C}$ and $M_{p\pi^-+\rm inv.}$ are optimized by maximizing the Punzi significance $= \frac{\epsilon}{1.5+\sqrt{B}}$ [43], where ϵ denotes the signal efficiency obtained from signal MC sample and B is the number of background events obtained from background MC samples.

5 Signal extraction

After the full event selection, the residual background is dominated by $J/\psi \to \bar{\Xi}^0(\to \bar{\Lambda}\pi^0)\,\Xi^0(\to \Lambda\pi^0)$ and $J/\psi \to \bar{\Sigma}^{*0}(\to \bar{\Lambda}\pi^0)\,\Sigma^{*0}(\to \Lambda\pi^0)$. Since the invisible particle should not deposit energy in the EMC, the total energy of all EMC showers excluding the ST π^0, denoted as $E_{\rm extra}$, provides powerful discrimination. The $E_{\rm extra}$ can be divided into two parts

$$E_{\rm extra} = E^{\rm DT\pi^0}_{\rm extra} + E^{\rm other}_{\rm extra}, \tag{5.1}$$

where $E^{\rm DT\pi^0}_{\rm extra}$ is the energy of the π^0 on the DT side, expected to be zero for signal events. The value of $E^{\rm DT\pi^0}_{\rm extra}$ in the background is obtained from MC simulation, whose modelling of the photon and electron interactions with the detector materials is sufficiently accurate. The $E^{\rm other}_{\rm extra}$ comes from other contributions, including from unrelated sources such as detector

JHEP05(2026)073

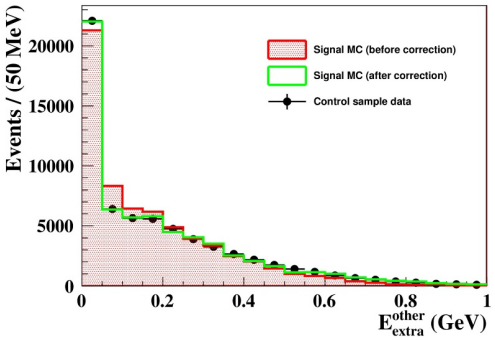

Figure 3. The $E^{\rm other}_{\rm extra}$ distribution. The red histogram represents the Signal MC before the correction, the green histogram represents the Signal MC after the correction, and the black dots with error bars represent the $J/\psi \to \bar{\Xi}^0(\to \bar{\Lambda}\pi^0)\Xi^0(\to \Lambda\pi^0)$ control sample.

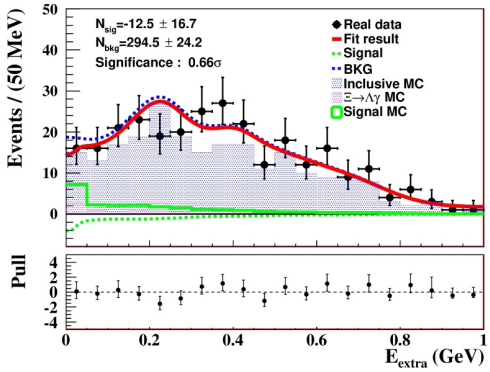

Figure 4. Fit on the $E_{\rm extra}$ distribution. The black dots with error bars represent the data sample, the red line represents the fitted curve, the green dashed line represents the signal component, and the blue dashed line represents the background component. The green histogram represents the signal MC sample (scaled according to the obtained upper limit of its BF), the blue histogram represents the inclusive MC sample, and the violet histogram represents the $\Xi^0 \to \Lambda\gamma$ MC sample. The bottom panel shows the pull values defined as $Pull^i = \frac{N^i_{\rm data} - N^i_{\rm fit}}{\sigma^i_{\rm data}}$, where $N^i_{\rm data}$ is the number of data events in the i-th bin, $N^i_{\rm fit}$ is the corresponding total number of fitted events, and $\sigma^i_{\rm data}$ is the statistical uncertainty of the data.

and electronic noises. After suppression of the induced showers through the isolation-angle requirements, the interactions of the $\bar{p}$ track with the detector materials are estimated to dominate the residual energy. Owing to the limitation of the GEANT4 in modelling the anti-proton interactions with detector materials, the raw simulated $E^{\rm other}_{\rm extra}$ disagrees with the distribution from the data, as shown in figure 3. Therefore, the shape of $E^{\rm other}_{\rm extra}$ is corrected using a data-driven approach based on a $J/\psi \to \bar{\Xi}^0(\to \bar{\Lambda}\pi^0)\Xi^0(\to \Lambda\pi^0)$ control sample. The contribution of $E^{\rm other}_{\rm extra}$ is assigned by sampling a random value from a shape template extracted from the control data sample, binned in the momentum and the polar angle of the anti-proton.

JHEP05(2026)073

A binned extended maximum likelihood fit is performed to the corrected distribution of $E_{\rm extra}$ to determine the signal yields $N_{\rm fit}$, as shown in figure 4. The probability density functions of signal and background are derived from the shape of the signal MC and inclusive MC simulation after the data-driven correction. The fitted yield $N_{\rm fit}$ is -12.5 ± 16.7. The peaking background from $\Xi^0 \to \Lambda\gamma$, with the expected yield $N_{\rm Peaking} = 8.5$ from a $\Xi^0 \to \Lambda\gamma$ MC sample, mimics the signal but is absent from the inclusive MC sample. The DT signal yield $N_{\rm DT}$ is obtained by subtracting the peaking background $N_{\rm Peaking}$ from the fitted yield $N_{\rm fit}$. The result indicates no significant excess of observed signal above the expected backgrounds.

6 Systematic uncertainties

The DT analysis technique cancels most systematic uncertainties related to the ST selection. The remaining systematic uncertainties are divided into multiplicative uncertainties and additive uncertainties.

The multiplicative systematic uncertainties arise from the MC generator, the intermediate BF, the peaking background, and the selection requirements on $\chi^2_{\rm 2C}$, $\cos\theta_{\rm inv.}$, $|\vec{P}_{\rm inv.}|$, $M_{p\pi^-+{\rm inv.}}$, $\chi^2_{3\gamma}$, and $\chi^2_{4\gamma}$. Adding the individual components in quadrature gives a total multiplicative systematic uncertainty of 9.5%, as summarized in table 1.

- *MC generator.* To study the uncertainty arising from the signal MC generator, the decay parameters α_{Ξ^0} used in the mDIY model are varied from 0 to -0.5 and +0.5 [40]. The largest efficiency difference of 5.0% between the alternative and nominal signal MC samples is assigned as the uncertainty.

- *Intermediate BF.* The uncertainty of $\mathcal{B}(\Lambda \to p\pi^-)$ from the PDG [36] is 0.8%.

- *Peaking background.* The uncertainty on the peaking background $\Xi^0 \to \Lambda\gamma$ is estimated to be 6.9%, combining the BF uncertainty quoted from the PDG [36] with the limited MC statistics.

- *Requirements on* $\chi^2_{\rm 2C}$, $\cos\theta_{\rm inv.}$, $|\vec{P}_{\rm inv.}|$, $M_{p\pi^-+{\rm inv.}}$, $\chi^2_{3\gamma}$, $\chi^2_{4\gamma}$. A control sample $J/\psi \to \bar{\Xi}^0\Xi^0$, where $\Xi^0 \to \Lambda\pi^0$ and $\bar{\Xi}^0 \to \Lambda\pi^0$, is used to study the selection requirements uncertainties. The same ST selections as those in section 3 are applied to the control sample. To suppress the background, further selections $M_{\rm bc} \in (1.304, 1.321)\,{\rm GeV}/c^2$ and $\chi^2_{4\gamma} < 100$ are applied. Specifically, the $\chi^2_{4\gamma} < 100$ requirement is omitted when studying the uncertainty associated with this specific criterion. Under the same selections, the efficiency differences between the MC and the data are taken as the corresponding uncertainties. The uncertainties from the $\chi^2_{\rm 2C}$, $\cos\theta_{\rm inv.}$, $|\vec{P}_{\rm inv.}|$, $M_{p\pi^-+{\rm inv.}}$, $\chi^2_{3\gamma}$, $\chi^2_{4\gamma}$ requirements are found to be 2.1%, 1.1%, 1.7%, 1.4%, 1.9% and 1.8%, respectively.

The additive systematic uncertainties mainly come from the bin width, the background shape and the signal shape. Since we perform the binned maximum-likelihood fit on the $E_{\rm extra}$ distribution using 20 MeV bin width, the uncertainty arising from the choice of bin width is considered by using alternative bin widths of 10 MeV and 40 MeV. To consider the influence of the fluctuations caused by the background shape, we change the smoothing parameter (ρ value) of the RooKeysPDF function from 1 to 2 or 3. The uncertainty associated with

JHEP05(2026)073

Sources	Relative systematic uncertainties (%)
MC generator	5.0
Intermediate BF	0.8
Peaking background	6.9
$\chi^2_{\rm 2C}$ requirement	2.1
$\cos\theta_{\rm inv.}$ requirement	1.1
$\lvert\vec{P}_{\rm inv.}\rvert$ requirement	1.7
$M_{p\pi^-+{\rm inv.}}$ requirement	1.4
$\chi^2_{\rm 3\gamma}$ requirement	1.9
$\chi^2_{\rm 4\gamma}$ requirement	1.8
Total	9.5

Table 1. Summary of the multiplicative systematic uncertainties for the BF measurements. The total value is calculated by summing up all sources in quadrature.

the signal shape is considered by replacing the nominal model with alternative models in which the decay-asymmetry parameter of $\Xi^0 \to \Lambda +$ invisible is varied between -0.5 and 0.5. We obtain an upper limit (UL) for each alternative case and take the most conservative UL as the final result.

7 Result

Since no significant signal is observed, we set the UL on $\mathcal{B}(\Xi^0 \to \Lambda +$ invisible) at the 90% confidence level (C.L.) after considering the systematic uncertainties. For each fixed signal yield, a BF value is obtained according to eq. (3.1), and a likelihood value is obtained from the fitting. We scan the signal yields 200 times by varying the number of events with a step size of 0.3 to obtain the likelihood distribution $\mathcal{L}_i$ and the maximum likelihood $\mathcal{L}_{\rm max}$. The relative likelihood $\mathcal{L}$ is defined as

$$\mathcal{L} = \frac{\mathcal{L}_i}{\mathcal{L}_{\rm max}}. \tag{7.1}$$

A Gaussian fit is performed to the distribution of the relative likelihood. Then we obtain a mean value and an uncertainty of the BF, denoted $\hat{\mathcal{B}}$ and $\sigma_{\mathcal{B}}$. The related likelihood function is

$$\mathcal{L}(\mathcal{B})_{\rm fit} \propto \exp\left[-\frac{(\mathcal{B}-\hat{\mathcal{B}})^2}{2\sigma^2_{\mathcal{B}}}\right]. \tag{7.2}$$

By following a method [44] which incorporates the systematic uncertainties into the UL of the BF, we obtain the smeared likelihood function,

$$\mathcal{L}(\mathcal{B})_{\rm smear} \propto \int_0^1 \exp\left[-\frac{(\epsilon\mathcal{B}/\hat{\epsilon}-\hat{\mathcal{B}})^2}{2\sigma^2_{\mathcal{B}}}\right] \times \frac{1}{\sqrt{2\pi}\sigma_{\rm sys}\hat{\epsilon}} \exp\left[-\frac{(\epsilon-\hat{\epsilon})^2}{2\sigma^2_{\rm sys}\hat{\epsilon}^2}\right] d\epsilon, \tag{7.3}$$

where $\hat{\epsilon}$ is the nominal efficiency and $\sigma_{\rm sys}$ denotes the multiplicative systematic uncertainty.

JHEP05(2026)073

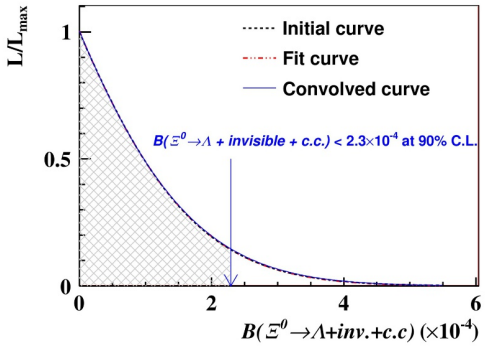

Figure 5. The distributions of the likelihood curves. The dotted-dashed black line is the initial curve, the dotted-dashed red line is the fit curve with a Gaussian function, and the solid blue line is the fit curve convolved with a Gaussian for systematic uncertainties. The blue arrow indicates the UL on BF at the 90% C.L.

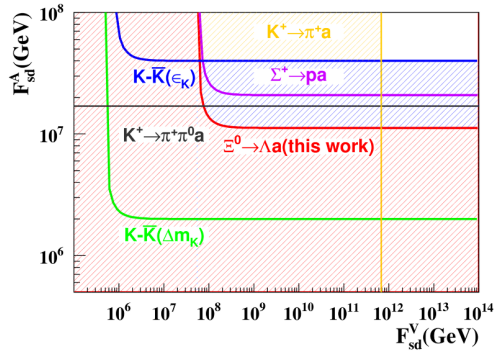

Figure 6. The 90% C.L. exclusion limits of $s \to d$ flavor-violating axion couplings obtained by various experiments, $\Sigma^+ \to pa$ [47], $K^+ \to \pi^+ a$ [46], $K^+ \to \pi^+\pi^0 a$ [48], $K - \bar{K}(\Delta m_K)$ [36], $K - \bar{K}(\epsilon_K)$ [49].

Also considering the additive systematic uncertainties detailed in section 6, we obtain the most conservative UL at the 90% C.L. on the BF to be $\mathcal{B}(\Xi^0 \to \Lambda + \text{invisible}) < 2.3 \times 10^{-4}$, as shown in figure 5. Under the hypothesis of a massless dark photon, the maximum allowed BF of $\Xi^0 \to \Lambda\gamma'$ is 1.2×10^{-4} [45], which remains consistent with our experimental bound. For the QCD axion, the vector coupling F^V_{sd} is already tightly constrained by $K^+ \to \pi^+ a$ [46] searches, as shown in figure 6. However, a lower bound of the axial-vectorial part F^A_{sd} is set using the UL obtained in this study, which is significantly better than the constraint from $K - \bar{K}$ mixing (Δm_K) [36] and competitive with that from searches for $\Sigma^+ \to pa$ [47], $K^+ \to \pi^+\pi^0 a$ [48] and measurements of the CP-violating parameter ϵ_K [49] in the kaon system, as shown in figure 6.

8 Summary

A massless particle beyond the SM is searched for in the Ξ^0 FCNC decay $\Xi^0 \to \Lambda + \text{invisible}$ for the first time, using $(1.0087 \pm 0.0044) \times 10^{10}$ J/ψ events collected with the BESIII detector.

JHEP05(2026)073

No significant signals are observed above the expected backgrounds. The UL on BF is set to be $\mathcal{B}(\Xi^0 \to \Lambda + \text{invisible}) < 2.3 \times 10^{-4}$ at the 90% C.L. after taking into account the systematic uncertainties. Throughout this paper, charge-conjugate processes are always implied. This result provides the first experimental constraint on this decay mode and imposes stringent limits on various new physics models involving a massless BSM particle.

Acknowledgments

The BESIII Collaboration thanks the staff of BEPCII (https://cstr.cn/31109.02.BEPC) and the IHEP computing center for their strong support. This work is supported in part by National Key R&D Program of China under Contracts Nos. 2023YFA1606000, 2023YFA1606704; National Natural Science Foundation of China (NSFC) under Contracts Nos. 11635010, 11935015, 11935016, 11935018, 12025502, 12035009, 12035013, 12061131003, 12192260, 12192261, 12192262, 12192263, 12192264, 12192265, 12221005, 12225509, 12235017, 12342502, 12361141819; the Chinese Academy of Sciences (CAS) Large-Scale Scientific Facility Program; the Strategic Priority Research Program of Chinese Academy of Sciences under Contract No. XDA0480600; CAS under Contract No. YSBR-101; 100 Talents Program of CAS; The Institute of Nuclear and Particle Physics (INPAC) and Shanghai Key Laboratory for Particle Physics and Cosmology; ERC under Contract No. 758462; German Research Foundation DFG under Contract No. FOR5327; Istituto Nazionale di Fisica Nucleare, Italy; Knut and Alice Wallenberg Foundation under Contracts Nos. 2021.0174, 2021.0299, 2023.0315; Ministry of Development of Turkey under Contract No. DPT2006K-120470; National Research Foundation of Korea under Contract No. NRF-2022R1A2C1092335; National Science and Technology fund of Mongolia; Polish National Science Centre under Contract No. 2024/53/B/ST2/00975; STFC (United Kingdom); Swedish Research Council under Contract No. 2019.04595; U.S. Department of Energy under Contract No. DE-FG02-05ER41374

Data Availability Statement. This article has no associated data or the data will not be deposited.

Code Availability Statement. This article has no associated code or the code will not be deposited.

References

[1] G. Buchalla, A.J. Buras and M.E. Lautenbacher, *Weak decays beyond leading logarithms*, *Rev. Mod. Phys.* **68** (1996) 1125 [hep-ph/9512380] [INSPIRE].

[2] J. Tandean, *Rare hyperon decays with missing energy*, *JHEP* **04** (2019) 104 [arXiv:1901.10447] [INSPIRE].

[3] R.D. Peccei and H.R. Quinn, *CP conservation in the presence of instantons*, *Phys. Rev. Lett.* **38** (1977) 1440 [INSPIRE].

JHEP05(2026)073

[4] R.D. Peccei and H.R. Quinn, *Constraints imposed by CP conservation in the presence of instantons*, *Phys. Rev. D* **16** (1977) 1791 [INSPIRE].

[5] S. Weinberg, *A new light boson?*, *Phys. Rev. Lett.* **40** (1978) 223 [INSPIRE].

[6] F. Wilczek, *Problem of strong P and T invariance in the presence of instantons*, *Phys. Rev. Lett.* **40** (1978) 279 [INSPIRE].

[7] H. Georgi, D.B. Kaplan and L. Randall, *Manifesting the invisible axion at low-energies*, *Phys. Lett. B* **169** (1986) 73 [INSPIRE].

[8] J. Preskill, M.B. Wise and F. Wilczek, *Cosmology of the invisible axion*, *Phys. Lett. B* **120** (1983) 127 [INSPIRE].

[9] L.F. Abbott and P. Sikivie, *A cosmological bound on the invisible axion*, *Phys. Lett. B* **120** (1983) 133 [INSPIRE].

[10] M. Dine and W. Fischler, *The not so harmless axion*, *Phys. Lett. B* **120** (1983) 137 [INSPIRE].

[11] J. Martin Camalich et al., *Quark flavor phenomenology of the QCD axion*, *Phys. Rev. D* **102** (2020) 015023 [arXiv:2002.04623] [INSPIRE].

[12] B.A. Dobrescu, *Massless gauge bosons other than the photon*, *Phys. Rev. Lett.* **94** (2005) 151802 [hep-ph/0411004] [INSPIRE].

[13] E. Gabrielli, B. Mele, M. Raidal and E. Venturini, *FCNC decays of standard model fermions into a dark photon*, *Phys. Rev. D* **94** (2016) 115013 [arXiv:1607.05928] [INSPIRE].

[14] M. He, X.-G. He, C.-K. Huang and G. Li, *Search for a heavy dark photon at future e^+e^- colliders*, *JHEP* **03** (2018) 139 [arXiv:1712.09095] [INSPIRE].

[15] L. Ackerman, M.R. Buckley, S.M. Carroll and M. Kamionkowski, *Dark matter and dark radiation*, *Phys. Rev. D* **79** (2009) 023519 [arXiv:0810.5126] [INSPIRE].

[16] BESIII collaboration, *Number of J/ψ events at BESIII*, *Chin. Phys. C* **46** (2022) 074001 [arXiv:2111.07571] [INSPIRE].

[17] BESIII collaboration, *Design and construction of the BESIII detector*, *Nucl. Instrum. Meth. A* **614** (2010) 345 [arXiv:0911.4960] [INSPIRE].

[18] C. Yu et al., *BEPCII performance and beam dynamics studies on luminosity*, in the proceedings of the *7th International Particle Accelerator Conference*, Busan, South Korea, May 08–13 (2016) [DOI:10.18429/JACoW-IPAC2016-TUYA01] [INSPIRE].

[19] BESIII collaboration, *Future physics programme of BESIII*, *Chin. Phys. C* **44** (2020) 040001 [arXiv:1912.05983] [INSPIRE].

[20] J. Lu, Y. Xiao and X. Ji, *Online monitoring of the center-of-mass energy from real data at BESIII*, *Radiat. Detect. Technol. Methods* **4** (2020) 337 [INSPIRE].

[21] J.-W. Zhang et al., *Suppression of top-up injection backgrounds with offline event filter in the BESIII experiment*, *Radiat. Detect. Technol. Methods* **6** (2022) 289 [INSPIRE].

[22] M.-H. Liao et al., *Experimental dataset from BESIII detector at Beijing electron–positron collider*, *Nucl. Sci. Tech.* **36** (2025) 218 [arXiv:2509.16066] [INSPIRE].

[23] X. Li et al., *Study of MRPC technology for BESIII endcap-TOF upgrade*, *Radiat. Detect. Technol. Methods* **1** (2017) 13 [INSPIRE].

[24] Y.-X. Guo et al., *The study of time calibration for upgraded end cap TOF of BESIII*, *Radiat. Detect. Technol. Methods* **1** (2017) 15 [INSPIRE].

JHEP05(2026)073

[25] P. Cao et al., *Design and construction of the new BESIII endcap time-of-flight system with MRPC technology*, *Nucl. Instrum. Meth. A* **953** (2020) 163053 [INSPIRE].

[26] GEANT4 collaboration, *GEANT4 — a simulation toolkit*, *Nucl. Instrum. Meth. A* **506** (2003) 250 [INSPIRE].

[27] K.-X. Huang et al., *Method for detector description transformation to Unity and application in BESIII*, *Nucl. Sci. Tech.* **33** (2022) 142 [arXiv:2206.10117] [INSPIRE].

[28] Z.-J. Li et al., *Visualization for physics analysis improvement and applications in BESIII*, *Front. Phys. (Beijing)* **19** (2024) 64201 [arXiv:2404.07951] [INSPIRE].

[29] T.-Z. Song et al., *Detector description conversion and visualization in Unity for high energy physics experiments*, *Front. Phys. (Beijing)* **21** (2026) 26201 [arXiv:2507.10261] [INSPIRE].

[30] Y.-T. Liang et al., *A uniform geometry description for simulation, reconstruction and visualization in the BESIII experiment*, *Nucl. Instrum. Meth. A* **603** (2009) 325 [INSPIRE].

[31] Z.-Y. You, Y.-T. Liang and Y.-J. Mao, *A method for detector description exchange among ROOT GEANT4 and GEANT3*, *Chin. Phys. C* **32** (2008) 572 [INSPIRE].

[32] S. Jadach, B.F.L. Ward and Z. Was, *Coherent exclusive exponentiation for precision Monte Carlo calculations*, *Phys. Rev. D* **63** (2001) 113009 [hep-ph/0006359] [INSPIRE].

[33] S. Jadach, B.F.L. Ward and Z. Was, *The precision Monte Carlo event generator K K for two fermion final states in e^+e^- collisions*, *Comput. Phys. Commun.* **130** (2000) 260 [hep-ph/9912214] [INSPIRE].

[34] D.J. Lange, *The EvtGen particle decay simulation package*, *Nucl. Instrum. Meth. A* **462** (2001) 152 [INSPIRE].

[35] R.-G. Ping, *Event generators at BESIII*, *Chin. Phys. C* **32** (2008) 599 [INSPIRE].

[36] Particle Data Group collaboration, *Review of particle physics*, *Phys. Rev. D* **110** (2024) 030001 [INSPIRE].

[37] J.C. Chen et al., *Event generator for J/ψ and $\psi(2S)$ decay*, *Phys. Rev. D* **62** (2000) 034003 [INSPIRE].

[38] R.-L. Yang, R.-G. Ping and H. Chen, *Tuning and Validation of the Lundcharm Model with J/ψ Decays*, *Chin. Phys. Lett.* **31** (2014) 061301 [INSPIRE].

[39] E. Barberio, B. van Eijk and Z. Was, *PHOTOS: a universal Monte Carlo for QED radiative corrections in decays*, *Comput. Phys. Commun.* **66** (1991) 115 [INSPIRE].

[40] BESIII collaboration, *Tests of CP symmetry in entangled $\Xi^0\bar{\Xi}^0$ pairs*, *Phys. Rev. D* **108** (2023) L031106 [arXiv:2305.09218] [INSPIRE].

[41] W.D. Li et al., *The BESIII offline software*, in *Proceeding of CHEP06*, S. Banerjee ed., Tata Institute of Fundamental Research, Mumbai, India (2006).

[42] BESIII collaboration, *Study of J/ψ and $\psi(3686) \to \Sigma(1385)^0\bar{\Sigma}(1385)^0$ and $\Xi^0\bar{\Xi}^0$*, *Phys. Lett. B* **770** (2017) 217 [arXiv:1612.08664] [INSPIRE].

[43] G. Punzi, *Sensitivity of searches for new signals and its optimization*, *eConf C* **030908** (2003) MODT002 [physics/0308063] [INSPIRE].

[44] X.-X. Liu, X.-R. Lü and Y.-S. Zhu, *Combined estimation for multi-measurements of branching ratio*, *Chin. Phys. C* **39** (2015) 103001 [arXiv:1505.01278] [INSPIRE].

[45] J.-Y. Su and J. Tandean, *Searching for dark photons in hyperon decays*, *Phys. Rev. D* **101** (2020) 035044 [arXiv:1911.13301] [INSPIRE].

JHEP05(2026)073

[46] E949 and E787 collaborations, *Measurement of the $K^+ \to \pi^+ \nu\bar{\nu}$ branching ratio*, *Phys. Rev. D* **77** (2008) 052003 [arXiv:0709.1000] [INSPIRE].

[47] BESIII collaboration, *Search for a massless particle beyond the Standard Model in the $\Sigma^+ \to p$ + invisible decay*, *Phys. Lett. B* **852** (2024) 138614 [arXiv:2312.17063] [INSPIRE].

[48] E787 collaboration, *Search for the decay $K^+ \to \pi^+ \pi^0$ neutrino anti-neutrino*, *Phys. Rev. D* **63** (2001) 032004 [hep-ex/0009055] [INSPIRE].

[49] UTfit collaboration, *New UTfit analysis of the unitarity triangle in the Cabibbo-Kobayashi-Maskawa scheme*, *Rend. Lincei Sci. Fis. Nat.* **34** (2023) 37 [arXiv:2212.03894] [INSPIRE].

JHEP05(2026)073

The BESIII collaboration

M. Ablikim[1], M. N. Achasov[4,d], P. Adlarson[83], X. C. Ai[89], C. S. Akondi[31A,31B], R. Aliberti[39], A. Amoroso[82A,82C], Q. An[79,65,†], Y. H. An[89], Y. Bai[63], O. Bakina[40], H. R. Bao[71], X. L. Bao[50], M. Barbagiovanni[82C], V. Batozskaya[1,49], K. Begzsuren[35], N. Berger[39], M. Berlowski[49], M. B. Bertani[30A], D. Bettoni[31A], F. Bianchi[82A,82C], E. Bianco[82A,82C], A. Bortone[82A,82C], I. Boyko[40], R. A. Briere[5], A. Brueggemann[76], D. Cabiati[82A,82C], H. Cai[84], M. H. Cai[42,l,m], X. Cai[1,65], A. Calcaterra[30A], G. F. Cao[1,71], N. Cao[1,71], S. A. Cetin[69A], X. Y. Chai[51,i], J. F. Chang[1,65], T. T. Chang[48], G. R. Che[48], Y. Z. Che[1,65,71], C. H. Chen[10], Chao Chen[1], G. Chen[1], H. S. Chen[1,71], H. Y. Chen[20], M. L. Chen[1,65,71], S. J. Chen[47], S. M. Chen[68], T. Chen[1,71], W. Chen[50], X. R. Chen[34,71], X. T. Chen[1,71], X. Y. Chen[12,h], Y. B. Chen[1,65], Y. Q. Chen[16], Z. K. Chen[66], J. Cheng[50], L. N. Cheng[48], S. K. Choi[11], X. Chu[12,h], G. Cibinetto[31A], F. Cossio[82C], J. Cottee-Meldrum[70], H. L. Dai[1,65], J. P. Dai[87], X. C. Dai[68], A. Dbeyssi[19], R. E. de Boer[3], D. Dedovich[40], C. Q. Deng[80], Z. Y. Deng[1], A. Denig[39], I. Denisenko[40], M. Destefanis[82A,82C], F. De Mori[82A,82C], E. Di Fiore[31A,31B], X. X. Ding[51,i], Y. Ding[44], Y. X. Ding[32], Yi. Ding[38], J. Dong[1,65], L. Y. Dong[1,71], M. Y. Dong[1,65,71], X. Dong[84], Z. J. Dong[66], M. C. Du[1], S. X. Du[89], Shaoxu Du[12,h], X. L. Du[12,h], Y. Q. Du[84], Y. Y. Duan[61], Z. H. Duan[47], P. Egorov[40,b], G. F. Fan[47], J. J. Fan[20], Y. H. Fan[50], J. Fang[1,65], Jin Fang[66], S. S. Fang[1,71], W. X. Fang[1], Y. Q. Fang[1,65,†], L. Fava[82B,82C], F. Feldbauer[3], G. Felici[30A], C. Q. Feng[79,65], J. H. Feng[16], L. Feng[42,l,m], Q. X. Feng[42,l,m], Y. T. Feng[79,65], M. Fritsch[3], C. D. Fu[1], J. L. Fu[71], Y. W. Fu[1,71], H. Gao[71], Xu Gao[38], Y. Gao[79,65], Y. N. Gao[51,i], Y. Y. Gao[32], Yunong Gao[20], Z. Gao[48], S. Garbolino[82C], I. Garzia[31A,31B], L. Ge[63], P. T. Ge[20], Z. W. Ge[47], C. Geng[66], E. M. Gersabeck[75], A. Gilman[77], K. Goetzen[13], J. Gollub[3], J. B. Gong[1,71], J. D. Gong[38], L. Gong[44], W. X. Gong[1,65], W. Gradl[39], S. Gramigna[31A,31B], M. Greco[82A,82C], M. D. Gu[56], M. H. Gu[1,65], C. Y. Guan[1,71], A. Q. Guo[34], H. Guo[55], J. N. Guo[12,h], L. B. Guo[46], M. J. Guo[55], R. P. Guo[54], X. Guo[55], Y. P. Guo[12,h], Z. Guo[79,65], A. Guskov[40,b], J. Gutierrez[29], J. Y. Han[79,65], T. T. Han[1], X. Han[79,65], F. Hanisch[3], K. D. Hao[79,65], X. Q. Hao[20], F. A. Harris[72], C. Z. He[51,i], K. K. He[17,47], K. L. He[1,71], F. H. Heinsius[3], C. H. Heinz[39], Y. K. Heng[1,65,71], C. Herold[67], P. C. Hong[38], G. Y. Hou[1,71], X. T. Hou[1,71], Y. R. Hou[71], Z. L. Hou[1], H. M. Hu[1,71], J. F. Hu[62,k], Q. P. Hu[79,65], S. L. Hu[12,h], T. Hu[1,65,71], Y. Hu[1], Y. X. Hu[84], Z. M. Hu[66], G. S. Huang[79,65], K. X. Huang[66], L. Q. Huang[34,71], P. Huang[47], X. T. Huang[55], Y. P. Huang[1], Y. S. Huang[66], T. Hussain[81], N. Hüsken[39], N. in der Wiesche[76], J. Jackson[29], Q. Ji[1], Q. P. Ji[20], W. Ji[1,71], X. B. Ji[1,71], X. L. Ji[1,65], Y. Y. Ji[1], L. K. Jia[71], X. Q. Jia[55], D. Jiang[1,71], H. B. Jiang[84], S. J. Jiang[10], X. S. Jiang[1,65,71], Y. Jiang[71], J. B. Jiao[55], J. K. Jiao[38], Z. Jiao[25], L. C. L. Jin[1], S. Jin[47], Y. Jin[73], M. Q. Jing[1,71], M. Q. Jing[56], X. M. Jing[71], T. Johansson[83], S. Kabana[36], X. L. Kang[10], X. S. Kang[44], B. C. Ke[89], V. Khachatryan[29], A. Khoukaz[76], O. B. Kolcu[69A], B. Kopf[3], L. Kröger[76], L. Krümmel[3], Y. Y. Kuang[80], M. Kuessner[3], X. Kui[1,71], N. Kumar[28], A. Kupsc[49,83], W. Kühn[41], Q. Lan[80], W. N. Lan[20], T. T. Lei[79,65], M. Lellmann[39], T. Lenz[39], C. Li[52], C. H. Li[46], C. K. Li[48], Chunkai Li[21], Cong Li[48], D. M. Li[89], F. Li[1,65], G. Li[1], H. B. Li[1,71], H. J. Li[20], H. L. Li[89], H. N. Li[62,k], H. P. Li[48],

JHEP05(2026)073

Hui Li[48], J. N. Li[32], J. S. Li[66], J. W. Li[55], K. Li[1], K. L. Li[42,l,m], L. J. Li[1,71], Lei Li[53], M. H. Li[48], M. R. Li[1,71], M. T. Li[55], P. L. Li[71], P. R. Li[42,l,m], Q. M. Li[1,71], Q. X. Li[55], R. Li[18,34], S. Li[89], S. X. Li[89], S. Y. Li[89], Shanshan Li[27,j], T. Li[55], T. Y. Li[48], W. D. Li[1,71], W. G. Li[1,†], X. Li[1,71], X. H. Li[79,65], X. K. Li[51,i], X. L. Li[55], X. Y. Li[1,9], X. Z. Li[66], Y. Li[20], Y. B. Li[85], Y. C. Li[66], Y. G. Li[71], Y. P. Li[38], Z. H. Li[42], Z. J. Li[66], Z. L. Li[89], Z. X. Li[48], Z. Y. Li[87], C. Liang[47], H. Liang[79,65], Y. F. Liang[60], Y. T. Liang[34,71], Z. Z. Liang[66], G. R. Liao[14], L. B. Liao[66], M. H. Liao[66], Y. P. Liao[1,71], J. Libby[28], A. Limphirat[67], C. C. Lin[61], C. X. Lin[34], D. X. Lin[34,71], T. Lin[1], B. J. Liu[1], B. X. Liu[84], C. Liu[38], C. X. Liu[1], F. Liu[1], F. H. Liu[59], Feng Liu[6], G. M. Liu[62,k], H. Liu[42,l,m], H. B. Liu[15], H. M. Liu[1,71], Huihui Liu[22], J. B. Liu[79,65], J. J. Liu[21], K. Liu[42,l,m], K. Y. Liu[44], Ke Liu[23], Kun Liu[80], L. Liu[42], L. C. Liu[48], Lu Liu[48], M. H. Liu[38], P. L. Liu[55], Q. Liu[71], S. B. Liu[79,65], T. Liu[1], W. M. Liu[79,65], W. T. Liu[43], X. Liu[42,l,m], X. K. Liu[42,l,m], X. L. Liu[12,h], X. P. Liu[12,h], X. Y. Liu[84], Y. Liu[42,l,m], Y. B. Liu[48], Yi Liu[89], Z. A. Liu[1,65,71], Z. D. Liu[85], Z. L. Liu[80], Z. Q. Liu[55], Z. X. Liu[1], Z. Y. Liu[42], X. C. Lou[1,65,71], H. J. Lu[25], J. G. Lu[1,65], X. L. Lu[16], Y. Lu[7], Y. H. Lu[1,71], Y. P. Lu[1,65], Z. H. Lu[1,71], C. L. Luo[46], J. R. Luo[66], J. S. Luo[1,71], M. X. Luo[88], T. Luo[12,h], X. L. Luo[1,65], Z. Y. Lv[23], X. R. Lyu[71,p], Y. F. Lyu[48], Y. H. Lyu[89], F. C. Ma[44], H. L. Ma[1], Heng Ma[27,j], J. L. Ma[1,71], L. L. Ma[55], L. R. Ma[73], Q. M. Ma[1], R. Q. Ma[1,71], R. Y. Ma[20], T. Ma[79,65], X. T. Ma[1,71], X. Y. Ma[1,65], Y. M. Ma[34], F. E. Maas[19], I. MacKay[77], M. Maggiora[82A,82C], S. Maity[34], S. Malde[77], Q. A. Malik[81], H. X. Mao[42,l,m], Y. J. Mao[51,i], Z. P. Mao[1], S. Marcello[82A,82C], A. Marshall[70], F. M. Melendi[31A,31B], Y. H. Meng[71], Z. X. Meng[73], G. Mezzadri[31A], H. Miao[1,71], T. J. Min[47], R. E. Mitchell[29], X. H. Mo[1,65,71], B. Moses[29], N. Yu. Muchnoi[4,d], J. Muskalla[39], Y. Nefedov[40], F. Nerling[19,f], H. Neuwirth[76], Z. Ning[1,65], S. Nisar[33,a], Q. L. Niu[42,l,m], W. D. Niu[12,h], Y. Niu[55], C. Normand[70], S. L. Olsen[11,71], Q. Ouyang[1,65,71], S. Pacetti[30B,30C], Y. Pan[63], A. Pathak[11], Y. P. Pei[79,65], M. Pelizaeus[3], G. L. Peng[79,65], H. P. Peng[79,65], X. J. Peng[42,l,m], Y. Y. Peng[42,l,m], K. Peters[13,f], K. Petridis[70], J. L. Ping[46], R. G. Ping[1,71], S. Plura[39], V. Prasad[38], L. Pöpping[3], F. Z. Qi[1], H. R. Qi[68], M. Qi[47], S. Qian[1,65], W. B. Qian[71], C. F. Qiao[71], J. H. Qiao[20], J. J. Qin[80], J. L. Qin[61], L. Q. Qin[14], L. Y. Qin[79,65], P. B. Qin[80], X. P. Qin[43], X. S. Qin[55], Z. H. Qin[1,65], J. F. Qiu[1], Z. H. Qu[80], J. Rademacker[70], K. Ravindran[74], C. F. Redmer[39], A. Rivetti[82C], M. Rolo[82C], G. Rong[1,71], S. S. Rong[1,71], F. Rosini[30B,30C], Ch. Rosner[19], M. Q. Ruan[1,65], N. Salone[49,r], A. Sarantsev[40,e], Y. Schelhaas[39], M. Schernau[36], K. Schoenning[83], M. Scodeggio[31A], W. Shan[26], X. Y. Shan[79,65], Z. J. Shang[42,l,m], J. F. Shangguan[17], L. G. Shao[1,71], M. Shao[79,65], C. P. Shen[12,h], H. F. Shen[1,9], W. H. Shen[71], X. Y. Shen[1,71], B. A. Shi[71], Ch. Y. Shi[87,c], H. Shi[79,65], J. L. Shi[8,q], J. Y. Shi[1], M. H. Shi[89], S. Y. Shi[80], X. Shi[1,65], H. L. Song[79,65], J. J. Song[20], M. H. Song[42], T. Z. Song[66], W. M. Song[38], Y. X. Song[51,i,n], Zirong Song[27,j], S. Sosio[82A,82C], S. Spataro[82A,82C], S. Stansilaus[77], F. Stieler[39], M. Stolte[3], S. S Su[44], G. B. Sun[84], G. X. Sun[1], H. Sun[71], H. K. Sun[1], J. F. Sun[20], K. Sun[68], L. Sun[84], R. Sun[79], S. S. Sun[1,71], T. Sun[57,g], W. Y. Sun[56], Y. C. Sun[84], Y. H. Sun[32], Y. J. Sun[79,65], Y. Z. Sun[1], Z. Q. Sun[1,71], Z. T. Sun[55], H. Tabaharizato[1], C. J. Tang[60],

JHEP05(2026)073

G. Y. Tang[1], J. Tang[66], J. J. Tang[79,65], L. F. Tang[43], Y. A. Tang[84], Z. H. Tang[1,71], L. Y. Tao[80], M. Tat[77], J. X. Teng[79,65], J. Y. Tian[79,65], W. H. Tian[66], Y. Tian[34], Z. F. Tian[84], I. Uman[69B], E. van der Smagt[3], B. Wang[66], Bin Wang[1], Bo Wang[79,65], C. Wang[42,l,m], Chao Wang[20], Cong Wang[23], D. Y. Wang[51,i], F. K. Wang[66], H. J. Wang[42,l,m], H. R. Wang[86], J. Wang[10], J. J. Wang[84], J. P. Wang[37], K. Wang[1,65], L. L. Wang[1], L. W. Wang[38], M. Wang[55], Mi Wang[79,65], N. Y. Wang[71], S. Wang[42,l,m], Shun Wang[64], T. Wang[12,h], W. Wang[66], W. P. Wang[39], X. F. Wang[42,l,m], X. L. Wang[12,h], X. N. Wang[1,71], Xin Wang[27,j], Y. Wang[1], Y. D. Wang[50], Y. F. Wang[1,9,71], Y. H. Wang[42,l,m], Y. J. Wang[79,65], Y. L. Wang[20], Y. N. Wang[50], Yanning Wang[84], Yaqian Wang[18], Yi Wang[68], Yuan Wang[18,34], Z. Wang[1,65], Z. L. Wang[2], Z. Q. Wang[12,h], Z. Y. Wang[1,71], Zhi Wang[48], Ziyi Wang[71], D. Wei[48], D. H. Wei[14], D. J. Wei[73], H. R. Wei[48], F. Weidner[76], H. R. Wen[34], S. P. Wen[1], U. Wiedner[3], G. Wilkinson[77], M. Wolke[83], J. F. Wu[1,9], L. H. Wu[1], L. J. Wu[20], Lianjie Wu[20], S. G. Wu[1,71], S. M. Wu[71], X. W. Wu[80], Z. Wu[1,65], H. L. Xia[79,65], L. Xia[79,65], B. H. Xiang[1,71], D. Xiao[42,l,m], G. Y. Xiao[47], H. Xiao[80], Y. L. Xiao[12,h], Z. J. Xiao[46], C. Xie[47], K. J. Xie[1,71], Y. Xie[55], Y. G. Xie[1,65], Y. H. Xie[6], Z. P. Xie[79,65], T. Y. Xing[1,71], D. B. Xiong[1], G. F. Xu[1], H. Y. Xu[2], Q. J. Xu[17], Q. N. Xu[32], T. D. Xu[80], X. P. Xu[61], Y. Xu[12,h], Y. C. Xu[86], Z. S. Xu[71], F. Yan[24], L. Yan[12,h], W. B. Yan[79,65], W. C. Yan[89], W. H. Yan[6], W. P. Yan[20], X. Q. Yan[12,h], Y. Y. Yan[67], H. J. Yang[57,g], H. L. Yang[38], H. X. Yang[1], J. H. Yang[47], R. J. Yang[20], X. Y. Yang[73], Y. Yang[12,h], Y. G. Yang[56], Y. H. Yang[48], Y. M. Yang[89], Y. Q. Yang[10], Y. Z. Yang[20], Youhua Yang[47], Z. Y. Yang[80], W. J. Yao[6], Z. P. Yao[55], M. Ye[1,65], M. H. Ye[9,†], Z. J. Ye[62,k], Junhao Yin[48], Z. Y. You[66], B. X. Yu[1,65,71], C. X. Yu[48], G. Yu[13], J. S. Yu[27,j], L. W. Yu[12,h], T. Yu[80], X. D. Yu[51,i], Y. C. Yu[89], Yongchao Yu[42], C. Z. Yuan[1,71], H. Yuan[1,71], J. Yuan[38], Jie Yuan[50], L. Yuan[2], M. K. Yuan[12,h], S. H. Yuan[80], Y. Yuan[1,71], C. X. Yue[43], Ying Yue[20], A. A. Zafar[81], F. R. Zeng[55], S. H. Zeng[70], X. Zeng[12,h], Y. J. Zeng[1,71], Yujie Zeng[66], Y. C. Zhai[55], Y. H. Zhan[66], B. L. Zhang[1,71], B. X. Zhang[1,†], D. H. Zhang[48], G. Y. Zhang[20], Gengyuan Zhang[1,71], H. Zhang[79,65], H. C. Zhang[1,65,71], H. H. Zhang[66], H. Q. Zhang[1,65,71], H. R. Zhang[79,65], H. Y. Zhang[1,65], Han Zhang[89], J. Zhang[66], J. J. Zhang[58], J. L. Zhang[21], J. Q. Zhang[46], J. S. Zhang[12,h], J. W. Zhang[1,65,71], J. X. Zhang[42,l,m], J. Y. Zhang[1], J. Z. Zhang[1,71], Jianyu Zhang[71], Jin Zhang[53], Jiyuan Zhang[12,h], L. M. Zhang[68], Lei Zhang[47], N. Zhang[38], P. Zhang[1,9], Q. Zhang[20], Q. Y. Zhang[38], Q. Z. Zhang[71], R. Y. Zhang[42,l,m], S. H. Zhang[1,71], S. N. Zhang[77], Shulei Zhang[27,j], X. M. Zhang[1], X. Y. Zhang[55], Y. T. Zhang[89], Y. H. Zhang[1,65], Y. P. Zhang[79,65], Yao Zhang[1], Yu Zhang[80], Yu Zhang[66], Z. Zhang[34], Z. D. Zhang[1], Z. H. Zhang[1], Z. L. Zhang[38], Z. X. Zhang[20], Z. Y. Zhang[84], Zh. Zh. Zhang[20], Zhilong Zhang[61], Ziyang Zhang[50], Ziyu Zhang[48], G. Zhao[1], J.-P. Zhao[71], J. Y. Zhao[1,71], J. Z. Zhao[1,65], L. Zhao[1], Lei Zhao[79,65], M. G. Zhao[48], R. P. Zhao[71], S. J. Zhao[89], Y. B. Zhao[1,65], Y. L. Zhao[61], Y. P. Zhao[50], Y. X. Zhao[34,71], Z. G. Zhao[79,65], A. Zhemchugov[40,b], B. Zheng[80], B. M. Zheng[38], J. P. Zheng[1,65], W. J. Zheng[1,71], W. Q. Zheng[10], X. R. Zheng[20], Y. H. Zheng[71,p], B. Zhong[46], C. Zhong[20], X. Zhong[45], H. Zhou[39,55,o], J. Q. Zhou[38], S. Zhou[6], X. Zhou[84], X. K. Zhou[6], X. R. Zhou[79,65], X. Y. Zhou[43], Y. X. Zhou[86], Y. Z. Zhou[20], A. N. Zhu[71],

JHEP05(2026)073

J. Zhu[48], K. Zhu[1], K. J. Zhu[1,65,71], K. S. Zhu[12,h], L. X. Zhu[71], Lin Zhu[20], S. H. Zhu[78], T. J. Zhu[12,h], W. D. Zhu[12,h], W. J. Zhu[1], W. Z. Zhu[20], Y. C. Zhu[79,65], Z. A. Zhu[1,71], X. Y. Zhuang[48], M. Zhuge[55], J. H. Zou[1], J. Zu[34]

[1] *Institute of High Energy Physics, Beijing 100049, People's Republic of China*
[2] *Beihang University, Beijing 100191, People's Republic of China*
[3] *Bochum Ruhr-University, D-44780 Bochum, Germany*
[4] *Budker Institute of Nuclear Physics SB RAS (BINP), Novosibirsk 630090, Russia*
[5] *Carnegie Mellon University, Pittsburgh, Pennsylvania 15213, U.S.A.*
[6] *Central China Normal University, Wuhan 430079, People's Republic of China*
[7] *Central South University, Changsha 410083, People's Republic of China*
[8] *Chengdu University of Technology, Chengdu 610059, People's Republic of China*
[9] *China Center of Advanced Science and Technology, Beijing 100190, People's Republic of China*
[10] *China University of Geosciences, Wuhan 430074, People's Republic of China*
[11] *Chung-Ang University, Seoul, 06974, Republic of Korea*
[12] *Fudan University, Shanghai 200433, People's Republic of China*
[13] *GSI Helmholtzcentre for Heavy Ion Research GmbH, D-64291 Darmstadt, Germany*
[14] *Guangxi Normal University, Guilin 541004, People's Republic of China*
[15] *Guangxi University, Nanning 530004, People's Republic of China*
[16] *Guangxi University of Science and Technology, Liuzhou 545006, People's Republic of China*
[17] *Hangzhou Normal University, Hangzhou 310036, People's Republic of China*
[18] *Hebei University, Baoding 071002, People's Republic of China*
[19] *Helmholtz Institute Mainz, Staudinger Weg 18, D-55099 Mainz, Germany*
[20] *Henan Normal University, Xinxiang 453007, People's Republic of China*
[21] *Henan University, Kaifeng 475004, People's Republic of China*
[22] *Henan University of Science and Technology, Luoyang 471003, People's Republic of China*
[23] *Henan University of Technology, Zhengzhou 450001, People's Republic of China*
[24] *Hengyang Normal University, Hengyang 421001, People's Republic of China*
[25] *Huangshan College, Huangshan 245000, People's Republic of China*
[26] *Hunan Normal University, Changsha 410081, People's Republic of China*
[27] *Hunan University, Changsha 410082, People's Republic of China*
[28] *Indian Institute of Technology Madras, Chennai 600036, India*
[29] *Indiana University, Bloomington, Indiana 47405, U.S.A.*
[30A] *INFN Laboratori Nazionali di Frascati, I-00044, Frascati, Italy*
[30B] *INFN Sezione di Perugia, I-06100, Perugia, Italy*
[30C] *University of Perugia, I-06100, Perugia, Italy*
[31A] *INFN Sezione di Ferrara, I-44122, Ferrara, Italy*
[31B] *University of Ferrara, I-44122, Ferrara, Italy*
[32] *Inner Mongolia University, Hohhot 010021, People's Republic of China*
[33] *Institute of Business Administration, Karachi,*
[34] *Institute of Modern Physics, Lanzhou 730000, People's Republic of China*
[35] *Institute of Physics and Technology, Mongolian Academy of Sciences, Peace Avenue 54B, Ulaanbaatar 13330, Mongolia*
[36] *Instituto de Alta Investigación, Universidad de Tarapacá, Casilla 7D, Arica 1000000, Chile*
[37] *Jiangsu Ocean University, Lianyungang 222000, People's Republic of China*
[38] *Jilin University, Changchun 130012, People's Republic of China*
[39] *Johannes Gutenberg University of Mainz, Johann-Joachim-Becher-Weg 45, D-55099 Mainz, Germany*
[40] *Joint Institute for Nuclear Research, 141980 Dubna, Moscow region, Russia*
[41] *Justus-Liebig-Universitaet Giessen, II. Physikalisches Institut, Heinrich-Buff-Ring 16, D-35392 Giessen, Germany*
[42] *Lanzhou University, Lanzhou 730000, People's Republic of China*
[43] *Liaoning Normal University, Dalian 116029, People's Republic of China*
[44] *Liaoning University, Shenyang 110036, People's Republic of China*

JHEP05(2026)073

[45] Longyan University, Longyan 364000, People's Republic of China
[46] Nanjing Normal University, Nanjing 210023, People's Republic of China
[47] Nanjing University, Nanjing 210093, People's Republic of China
[48] Nankai University, Tianjin 300071, People's Republic of China
[49] National Centre for Nuclear Research, Warsaw 02-093, Poland
[50] North China Electric Power University, Beijing 102206, People's Republic of China
[51] Peking University, Beijing 100871, People's Republic of China
[52] Qufu Normal University, Qufu 273165, People's Republic of China
[53] Renmin University of China, Beijing 100872, People's Republic of China
[54] Shandong Normal University, Jinan 250014, People's Republic of China
[55] Shandong University, Jinan 250100, People's Republic of China
[56] Shandong University of Technology, Zibo 255000, People's Republic of China
[57] Shanghai Jiao Tong University, Shanghai 200240, People's Republic of China
[58] Shanxi Normal University, Linfen 041004, People's Republic of China
[59] Shanxi University, Taiyuan 030006, People's Republic of China
[60] Sichuan University, Chengdu 610064, People's Republic of China
[61] Soochow University, Suzhou 215006, People's Republic of China
[62] South China Normal University, Guangzhou 510006, People's Republic of China
[63] Southeast University, Nanjing 211100, People's Republic of China
[64] Southwest University of Science and Technology, Mianyang 621010, People's Republic of China
[65] State Key Laboratory of Particle Detection and Electronics, Beijing 100049, Hefei 230026, People's Republic of China
[66] Sun Yat-Sen University, Guangzhou 510275, People's Republic of China
[67] Suranaree University of Technology, University Avenue 111, Nakhon Ratchasima 30000, Thailand
[68] Tsinghua University, Beijing 100084, People's Republic of China
[69A] Turkish Accelerator Center Particle Factory Group Istinye University, 34010, Istanbul, Turkey
[69B] Turkish Accelerator Center Particle Factory Group, Near East University, Nicosia, North Cyprus, 99138, Mersin 10, Turkey
[70] University of Bristol, H H Wills Physics Laboratory, Tyndall Avenue, Bristol, BS8 1TL, U.K.
[71] University of Chinese Academy of Sciences, Beijing 100049, People's Republic of China
[72] University of Hawaii, Honolulu, Hawaii 96822, U.S.A.
[73] University of Jinan, Jinan 250022, People's Republic of China
[74] University of La Serena, Av. Raúl Bitrán 1305, La Serena, Chile
[75] University of Manchester, Oxford Road, Manchester, M13 9PL, United Kingdom
[76] University of Muenster, Wilhelm-Klemm-Strasse 9, 48149 Muenster, Germany
[77] University of Oxford, Keble Road, Oxford OX13RH, United Kingdom
[78] University of Science and Technology Liaoning, Anshan 114051, People's Republic of China
[79] University of Science and Technology of China, Hefei 230026, People's Republic of China
[80] University of South China, Hengyang 421001, People's Republic of China
[81] University of the Punjab, Lahore-54590, Pakistan
[82A] University of Turin, I-10125, Turin, Italy
[82B] University of Eastern Piedmont, I-15121, Alessandria, Italy
[82C] INFN, I-10125, Turin, Italy
[83] Uppsala University, Box 516, SE-75120 Uppsala, Sweden
[84] Wuhan University, Wuhan 430072, People's Republic of China
[85] Xi'an Jiaotong University, No.28 Xianning West Road, Xi'an, Shaanxi 710049, P.R. China
[86] Yantai University, Yantai 264005, People's Republic of China
[87] Yunnan University, Kunming 650500, People's Republic of China
[88] Zhejiang University, Hangzhou 310027, People's Republic of China
[89] Zhengzhou University, Zhengzhou 450001, People's Republic of China

[†] Deceased.
[a] Also at Bogazici University, 34342 Istanbul, Turkey.

JHEP05(2026)073

[b] Also at the Moscow Institute of Physics and Technology, Moscow 141700, Russia.
[c] Also at the Functional Electronics Laboratory, Tomsk State University, Tomsk, 634050, Russia.
[d] Also at the Novosibirsk State University, Novosibirsk, 630090, Russia.
[e] Also at the NRC "Kurchatov Institute", PNPI, 188300, Gatchina, Russia.
[f] Also at Goethe University Frankfurt, 60323 Frankfurt am Main, Germany.
[g] Also at Key Laboratory for Particle Physics, Astrophysics and Cosmology, Ministry of Education; Shanghai Key Laboratory for Particle Physics and Cosmology; Institute of Nuclear and Particle Physics, Shanghai 200240, People's Republic of China.
[h] Also at Key Laboratory of Nuclear Physics and Ion-beam Application (MOE) and Institute of Modern Physics, Fudan University, Shanghai 200443, People's Republic of China.
[i] Also at State Key Laboratory of Nuclear Physics and Technology, Peking University, Beijing 100871, People's Republic of China.
[j] Also at School of Physics and Electronics, Hunan University, Changsha 410082, China.
[k] Also at Guangdong Provincial Key Laboratory of Nuclear Science, Institute of Quantum Matter, South China Normal University, Guangzhou 510006, China.
[l] Also at MOE Frontiers Science Center for Rare Isotopes, Lanzhou University, Lanzhou 730000, People's Republic of China.
[m] Also at Lanzhou Center for Theoretical Physics, Lanzhou University, Lanzhou 730000, People's Republic of China.
[n] Also at Ecole Polytechnique Federale de Lausanne (EPFL), CH-1015 Lausanne, Switzerland.
[o] Also at Helmholtz Institute Mainz, Staudinger Weg 18, D-55099 Mainz, Germany.
[p] Also at Hangzhou Institute for Advanced Study, University of Chinese Academy of Sciences, Hangzhou 310024, China.
[q] Also at Applied Nuclear Technology in Geosciences Key Laboratory of Sichuan Province, Chengdu University of Technology, Chengdu 610059, People's Republic of China.
[r] Currently at University of Silesia in Katowice, Institute of Physics, 75 Pulku Piechoty 1, 41-500 Chorzow, Poland.

JHEP05(2026)073